

Transient thermography using evanescent microwave microscope

M. Tabib-Azar^{a)}

Electrical Engineering and Computer Science Department, Macromolecular Science Department, and Physics Department, Case Western Reserve University, Cleveland, Ohio 44106

R. Ciocan

Electrical Engineering and Computer Science Department, Case Western Reserve University, Cleveland, Ohio 44106

G. Ponchak

NASA Lewis Research Center, Cleveland, Ohio

S. R. LeClair

Air Force Research Laboratory, Materials and Manufacturing Directorate, Wright-Patterson Air Force Base, Ohio

(Received 3 March 1999; accepted for publication 21 April 1999)

Very high spatial resolution thermography is of great importance in electronics, biology, and in many other situations where local variations in temperature are needed to study heat dissipation or to monitor metabolism rate which can be directly related to the heat production. Infrared imaging techniques probably are the best way of obtaining thermal maps of large structures. However, the spatial resolution of infrared imaging techniques is limited to a few 100 μm and their temperature resolution is usually around 0.1 K. Here we report on a new evanescent microwave method that is capable of mapping temperature distributions with $\approx 1 \mu\text{m}$ spatial resolution. The temperature sensitivity of this probe was better than 0.1 V/K with a minimum detectable signal of 0.01 K with a response time faster than 1 μs . © 1999 American Institute of Physics. [S0034-6748(99)01308-8]

I. INTRODUCTION

Thermography with a high spatial resolution is of importance in many different areas. In microelectronics, it can be used to monitor thermal buildup and heat dissipation at the site of an electronic device. Such a monitoring capability is of importance in validating the thermal design of the device and it can be used to provide a feedback to modify the device structure. In biology, production of heat is directly related to the cell's metabolism and monitoring the temperature at the cell surface can be used to monitor its internal activity.

The main objective of this work is to discuss the application of the evanescent microwave probe (EMP) to measure local temperature with very high spatial and temperature resolutions nondestructively and nonintrusively. The EMP technique has been previously applied in nondestructive characterization of materials, and to the best of our knowledge the present work reports its applications in transient thermography for the first time. It is well known that the evanescent electromagnetic fields can be used to surpass the Abbe barrier in microscopy and to resolve objects much smaller than the wavelength of the excitation fields.^{1–13} In a series of recent articles,^{4–13} we have shown that a record resolution of $\lambda/750\,000$, which at 1 GHz results in 0.4 μm lateral resolution, can be obtained using evanescent microwave probes.⁶ Local probes, such as the scanning tunneling microscope (STM), atomic force microscope (AFM), scanning near-field optical microscope (SNOM), and various microwave near-field microscopes, have become quite popular

and drawn the attention of many researchers in recent years.

Evanescent wave imaging methods are quite powerful, and most of the recent scanning techniques with atomic or near atomic resolutions use some form of evanescent field phenomena. STM, for example, uses evanescent electronic wave functions to image atoms at the surface of *metals* or other *conducting materials*. SNOM uses evanescent optical fields to image variations in the refractive index or optical *absorption* with spatial resolution of 50–100 Å (this is approximately $\lambda/100$, with $\lambda \approx 5000\text{--}10\,000 \text{ Å}$). AFM uses interactions between near-field electronic wave functions and atomic cores to image atoms at the surface of insulators. In all these methods the spatial resolution is essentially limited by noise in the system for a given probe tip geometry and sensing method.

According to our previous findings, a well-designed two-dimensional (2D) stripline microwave probe should detect metallic features of less than 0.1 μm size in a dielectric background or dielectric lines of the same feature size in a metallic background at 1 GHz.⁵ The spatial resolution of the probe was theoretically found to be directly proportional to its tip size, and it is strongly affected by the distance between the tip and the sample. The conductivity resolution of this probe was estimated to be $10^{-2}\sigma_s$ in metals and $10^{-4}\sigma_s$ in semiconductors, and its permittivity resolution is $10^{-3}\epsilon_s$ in dielectrics. Experimentally, we have found a spatial resolution of $\lambda/750\,000$ (0.4 μm) and conductivity resolution of $10^{-1}\sigma_s$ in metals, $10^{-4}\sigma_s$ in semiconductors, and $10^{-3}\epsilon_s$ in dielectrics at 1 GHz.⁵

^{a)}Electronic mail: mxt7@po.cwru.edu

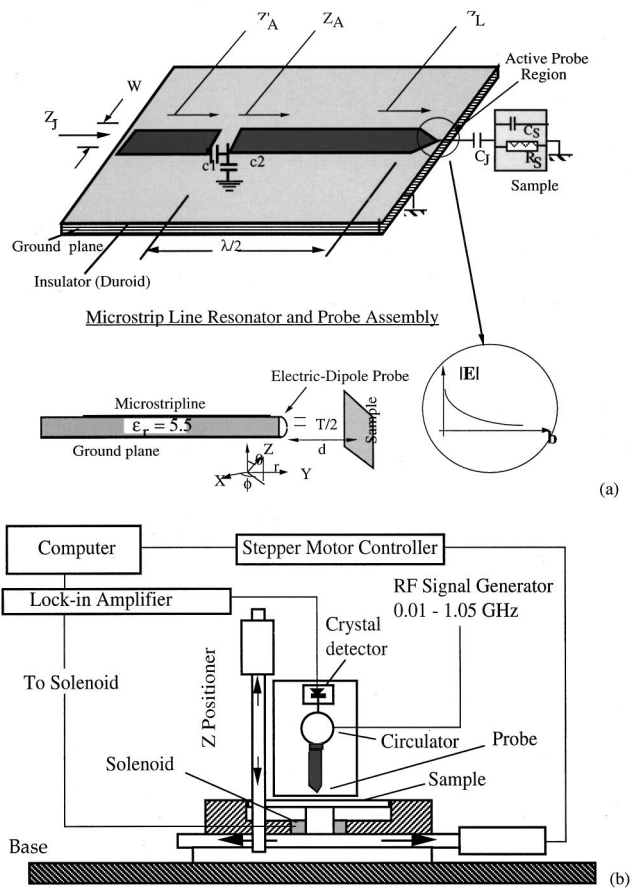


FIG. 1. (a) Evanescent microwave probe. (b) Experimental setup.

II. PRINCIPLE OF OPERATION

Figure 1 shows the EMP geometry used in our work. The resonator region is terminated by a tapered tip and the tip is positioned and scanned over a sample. The presence of the sample changes the resonance as shown in Fig. 2. The easiest method is to measure the change in the reflection coefficient of the resonator at a fixed operation frequency. To achieve the largest possible sensitivity in this method, the operation frequency should be chosen carefully. If the per-

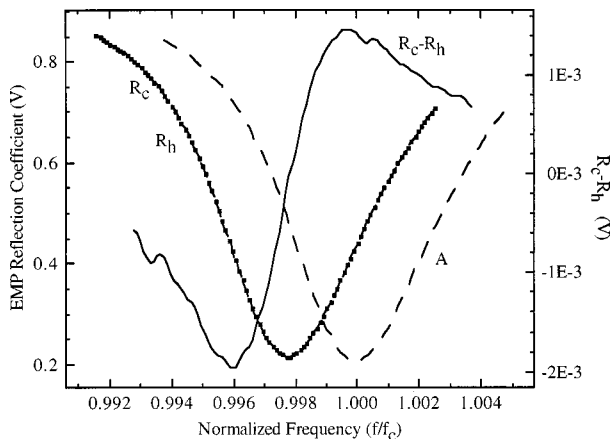


FIG. 2. (a) Two EMP spectra obtained with (R) and without (A) a resistive sample in front of the probe. The difference between these two spectra ($R-A$) and the difference spectra between cold and heated resistive sample (R_c-R_h) are also shown. The resonance frequency (f_c) was 893 MHz.

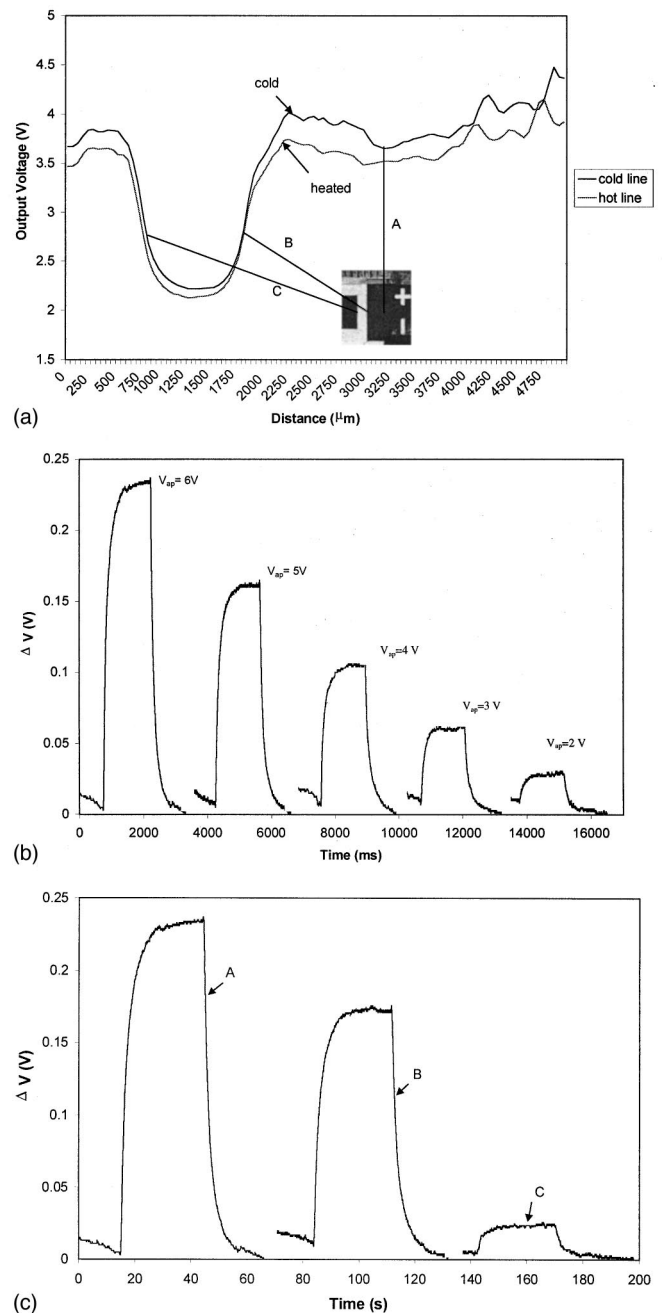


FIG. 3. (a) EMP scans of a resistor strip shown in the inset. The resistor was used as a heater and the EMP scans were obtained when the resistor was cold and after the resistor was heated by passing 5 mA at 2 V across it. (b) EMP response as a function of time as the heater was excited with various voltage pulses indicated in the figure. The EMP was located at point "A" on the resistor as shown in (a) inset. (c) EMP time response to a 2 V excitation applied to the heater at three different locations on the "A," "B," and "C" on the strip. These locations are shown in (a) inset.

turbation by the sample is not very large, the operation frequency corresponding to the maximum probe sensitivity can be obtained by differentiating the reflection spectrum with respect to the frequency. Figure 2 also shows the change in the resonator's reflection spectrum when the temperature of resistive sample placed near the tip was increased by 0.1 K.

Given a change in the reflection coefficient of ΔS_{11} per a small perturbation in temperature of ΔT of a sample placed in the vicinity of the probe, we can detect ΔS_{11} only if it is

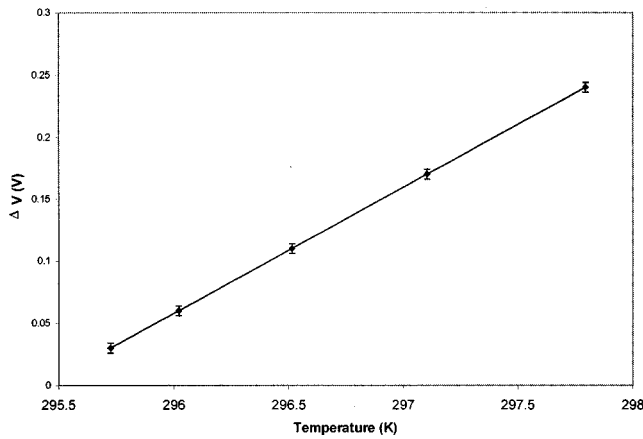


FIG. 4. The steady-state EMP output as a function of temperature of the heating element. The experimental dependence of the EMP voltage (ΔV) was $29.97 + 0.1014 T$ as determined from the above graph. The error bar of ΔV , obtained from run to run, was ± 0.004 V.

equal or larger than the noise level in the system [Fig. 1(b)]. This requirement of signal-to-noise ratio (SNR) of unity is an arbitrary requirement since it can be improved by using synchronous detection methods discussed elsewhere. Here, we assume SNR of unity. As shown in Fig. 2, the detected signal ΔS_{11} can be related to the slope of the resonator at f_x (f_x is the operation frequency that is kept fixed throughout the measurement) using the following relationship:⁵

$$\Delta S_{11} \approx \left. \frac{\Delta S_{11}}{\Delta f} \right|_{f_x} \times \Delta f. \quad (1)$$

Noting that the slope $(\Delta S_{11}/\Delta f)_{f_x}$ is the sensitivity of the resonator at f_x , we denote it by S_x . Furthermore, the minimum-detectable signal (MDS) is defined as the smallest change in the input (i.e., the measurand) that produces an output ($\Delta V_{\text{out}} = \Delta S_{11} V_{\text{in}}$) equal to the rms value of the noise (V_{nrms}). We note that in the case of a sample where its conductivity changes by $\Delta\sigma$ in response to a ΔT change in its temperature, ΔS_{11} can be written as

$$\frac{\Delta S_{11}}{\Delta T} = \frac{\Delta S_{11}}{\Delta f} \times \frac{\Delta f}{\Delta\sigma} \times \frac{\Delta\sigma}{\Delta T} \equiv S_x \times S_f \times S_{sT}, \quad (2)$$

where S_x is the frequency sensitivity of the resonator ($= \Delta S_{11}/\Delta f$), S_f is the shift in the resonator resonance per unit change in the conductivity ($= \Delta f/\Delta\sigma$) of a sample placed near the tip, and S_{sT} is the temperature sensitivity of the sample ($= \Delta\sigma/\Delta T$). Thus, for MDS we can write

$$\text{MDS} = \Delta T = \frac{\Delta S_{11}}{S_x \times S_f \times S_{sT}} \equiv \frac{V_{\text{nrms}}/V_{\text{in}}}{S_x \times S_f \times S_{sT}}, \quad (3)$$

where ΔT is the smallest detectable change in the temperature of the sample. Equation (3) clearly shows that to improve MDS, S_x and S_f , and S_{sT} should be maximized. S_x is related to the quality factor of the resonator while S_f is determined by the physical interaction between the evanescent fields and the sample as discussed in Ref. 5. S_{sT} is given by the conduction process in the sample and in the case of extrinsic silicon it is proportional to -0.2σ S/cm K near the room temperature. In the case of intrinsic semiconductors,

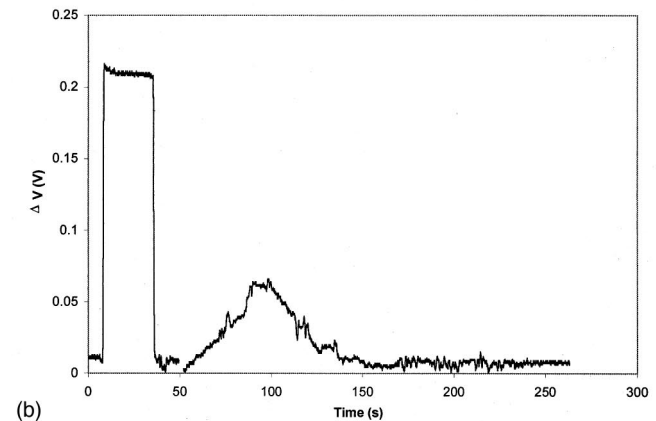
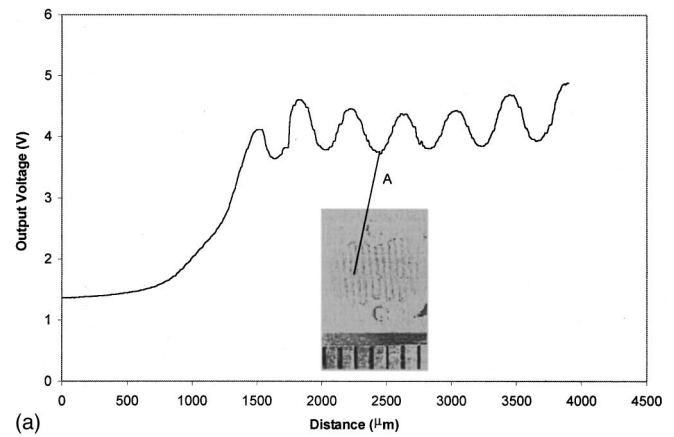


FIG. 5. (a) EMP scan over the photoresistor shown in the inset. (b) Time response of the EMP at location "A" over the photoresistor to an optical pulse (the first part of the response) and to a thermal pulse that was generated in the photoresistor by applying a voltage pulse of 6 V (current was 40 mA).

S_{sT} is exponentially proportional to temperature. In the case of metals it is negative and it is in the range of -0.001σ S/cm K near room temperature. Insulators are similar to intrinsic semiconductors.

In our case, the V_{nrms} was around 4 mV, V_{in} was 22 V, S_x was around 5×10^{-8} , S_f was 8×10^8 Hz/S/cm, and S_{sT} was 0.01 S/cm K. These values result in a minimum detectable temperature (signal) of 0.5×10^{-3} K.

III. EXPERIMENTAL PROCEDURE AND DATA

The experimental setup is shown in Fig. 1(b) and it is similar to the setup previously reported.³⁻¹³ It consists of a microwave resonator coupled to a feedline [Fig. 1(a)] and connected to a circulator. The circulator is also connected to a 0.01–1.05 GHz signal generator, and to a crystal microwave detector. The detector output is a dc voltage proportional to the magnitude of the reflected wave. This voltage is fed to an amplifier and thence to a lock-in amplifier. The probe is mounted vertically over an x - y stage [Fig. 1(b)]. Both the x - y stage, and the frequency generator, were controlled by a computer. The computer also acquires data from the lock-in amplifier. In synchronous measurements, either the probe or the sample is vibrated at ≈ 100 Hz. Although a bit more involved, both from the design and construction

points of view, vibrating the probe is better than vibrating the sample. Specially, in the case of a large sample, it is not possible to uniformly vibrate the sample without affecting the probe performance.

During measurements the sample was fixed on the x - y stage. To improve the spatial resolution of the EMP, a wire with a pointed etched tip is usually attached to the tapered portion of the resonator.⁶ We have shown that the EMP's spatial resolution is directly determined by the geometry of this wire's tip, i.e., a smaller tip improves spatial resolution. Moreover, the tip-to-sample distance should be made as small as possible to achieve very high spatial resolutions.

In Fig. 3(a) two EMP scans over a resistive strip are shown. One of these scans was obtained while the strip was at room temperature (the so-called "cold" scan) and the second scan was obtained while applying 2 V to the resistive strip (the so-called "heated" scan). The optical micrograph of the strip is shown in the Fig. 3 inset. Figure 3(b) shows the EMP responses at point "A" on the strip for different excitation voltages. Figure 3(c) shows the EMP responses at three different positions on the sample for 2 V excitation applied to the resistive strip. As the EMP was moved away from the strip, the temperature variations became smaller as can also be seen from the EMP scans shown in Fig. 3(a).

In all the above transient measurements the EMP response time was faster than 1 μ s as reported in Ref. 5. The EMP's operation frequency is around 1 GHz and its response is mainly limited by the bandwidth of the detector and subsequent amplifiers that typically have larger than 1 MHz bandwidth. Hence, all the transients in the EMP response curves are due to the thermal response of the material.

Figure 4 shows the steady-state EMP output as a function of the strip's temperature. This figure was calibrated by measuring the strip's temperature at different excitation voltages using a precision GaAs P - N diode temperature sensor. The temperature sensitivity of EMP in this case was around 0.10 V/K (or V/K) and the rms voltage noise was 4 mV. The resulting minimum detectable temperature change was 0.08 K.

In Fig. 5 an EMP scan over a photoresistor is shown. At point "A" at the surface of this photoresistor, shown in the Fig. 5 inset, the EMP response as a function time was recorded to monitor the optical and thermal responses of the photoresistor. These responses are shown in Fig. 5(b). The EMP response starting near $t=0$ is due to the optical response of the photoresistor. The second and more shallow EMP response was obtained when the photoresistor was excited by a 6 V pulse (40 mA was drawn by the resistor). These scans clearly show the ability of EMP in monitoring various processes that may take place inside the semiconducting material.

Figures 3–5 clearly demonstrate the capability of EMP in performing temporal and spatial thermography with very

high spatial and temperature resolutions. The spatial resolution of the EMP is shown to be around 0.4 μ m at 1 GHz. In the case of temperature maps, such a high spatial resolution may not be necessary since the thermal diffusion process inevitably results in more diffuse temperature profiles. This is particularly true in the case of highly thermally conducting substrates such as Si, SiC, or diamond (C).

Along with the conductivity of a sample, some of its other parameters may vary as a function of temperature. The real part of permittivity and any volumetric measures will also vary as a function of temperature and, hence, will contribute to the EMP signal. However, in most cases the conductivity variations as a function of temperature usually overshadow these other contributions.

Although we mentioned possible applications of EMP thermography in biology, we did not include any experimental results regarding biological specimens in the present work. These other applications can be viewed as natural and obvious extensions of the present studies.^{8–13}

We demonstrated the application of the evanescent microwave probes in performing transient and steady-state thermography of semiconducting materials and devices for the first time. The sensitivity of the EMP probe in detecting temperature variations was determined by three factors. These factors included the sensitivity of the EMP's resonator to a change in its operation frequency, to the interaction mechanisms between the probe and the sample, and to the temperature coefficient of the samples's conductivity. In the case of a 2.5×10^{-3} S/cm, the EMP's temperature sensitivity was found to be 0.1 V/K and its response time was faster than 1 μ s.

¹H. A. Bethe, Phys. Rev. **66**, 163 (1944).

²R. F. Soohoo, J. Appl. Phys. **33**, 1276 (1962).

³E. A. Ash and G. Nicholls, Nature (London) **237**, 510 (1972).

⁴M. Tabib-Azar, N. S. Shoemaker, and S. Harris, Meas. Sci. Technol. **4**, 583 (1993).

⁵M. Tabib-Azar, G. Ponchak, and S. LeClair, Rev. Sci. Instrum. **70**, 1 (1999).

⁶M. Tabib-Azar, D.-P. Su, A. Pohar, S. R. LeClair, and G. Ponchak, Rev. Sci. Instrum. **70**, 1725 (1999).

⁷G. E. Ponchak, A. Akinwande, and M. Tabib-Azar, Accepted for presentation at the Microwave Theory and Techniques Symposium (1999).

⁸M. Tabib-Azar, M. Mozayeni-Azar, S.-H. You, D.-P. Su, and L. J. Katz, presented at the International Association of Dental Research (IADR), Vancouver, BC, 1999.

⁹J. L. Katz, P. S. Pathak, S. Bumrerraj, and M. Tabib-Azar, presented at the 20th Annual International Conference of IEEE Engineering in Medicine and Biology Society, 1998.

¹⁰P. Pathak, M. Tabib-Azar, and G. Ponchak, presented at the International Conference of Non-Destructive Testing, Anaheim, CA, 1998.

¹¹J. L. Katz, M. Tabib-Azar, S. Bumrerraj, and P. S. Pathak, IADR, Nice, France, June 24–27, 1998.

¹²J. L. Katz, M. Tabib-Azar, S. Bumrerraj, and P. S. Pathak, presented at the The Third World Congress of Biomechanics, August 2–8, Hokkaido University, Sapporo, Japan, 1998.

¹³J. L. Katz, M. Tabib-Azar, S. Bumrerraj, and P. S. Pathak, presented at the WCB'98 Congress, Toyonaka, Osaka, Japan, 1998.